Macromolecules
ARTICLE

Macromolecules **2010**, *43*, 5195–5204 **5195**
DOI: 10.1021/ma100552v

End-Linked Semifluorinated Amphiphilic Polymer Conetworks: Synthesis by Sequential Reversible Addition−Fragmentation Chain Transfer Polymerization and Characterization

Kyriaki S. Pafiti,[†] Elena Loizou,[†] Costas S. Patrickios,*[,†] and Lionel Porcar[‡]

[†]*Department of Chemistry, University of Cyprus, P.O. Box 20537, 1678 Nicosia, Cyprus, and*
[‡]*Institute Max von Laue-Paul Langevin, BP 156, F-38042 Grenoble Cedex 9, France*

Received March 11, 2010; Revised Manuscript Received May 1, 2010

ABSTRACT: One-pot, sequential reversible addition−fragmentation chain transfer (RAFT) polymerization was employed for the preparation of five end-linked semifluorinated amphiphilic polymer conetworks based on 2,2,2-trifluoroethyl methacrylate (TFEMA, hydrophobic monomer) and 2-(dimethylamino)ethyl methacrylate (DMAEMA, hydrophilic monomer). 1,4-Bis[2-(thiobenzoylthio)prop-2-yl]benzene (1,4-BTBTPB) was used as the chain transfer agent, while ethylene glycol dimethacrylate (EGDMA) served as the cross-linker. Three of the end-linked conetworks were based on ABA triblock copolymers with polyDMAEMA midblocks with degrees of polymerization (DPs) of 50 and polyTFEMA end-blocks with overall polyTFEMA DPs of 25, 50, and 75. The fourth end-linked amphiphilic polymer conetwork was based on an equimolar BAB triblock copolymer with a polyTFEMA midblock and an overall copolymer DP of 100. The last end-linked conetwork was based on a statistical copolymer. A randomly cross-linked conetwork was also prepared by the simultaneous terpolymerization of the two comonomers (equimolar) and the cross-linker. The molecular weights and compositions of all the polymer precursors to the conetworks were characterized using gel permeation chromatography and ^{1}H NMR spectroscopy, respectively. The conetworks were characterized in terms of their degrees of swelling (DS) in THF and in water as a function of the solution pH. All conetworks swelled more in acidic than in pure water due to the ionization of the DMAEMA units in acidic water. The low pH aqueous DS of the statistical copolymer-based end-linked conetwork was higher than those of its triblock copolymer counterparts due to lack of microphase separation within the former conetwork. Finally, the microphase separation of the amphiphilic conetworks in deuterium oxide was investigated using small-angle neutron scattering which indicated a distance between the hydrophobic scattering centers of about 15 nm.

Introduction

Amphiphilic polymer conetworks (APCNs) represent a new class of polymeric materials consisting of chemically cross-linked hydrophilic and hydrophobic units.[1−4] Since their introduction in the late 1980s,[5−7] APCNs have been attracting increasing attention, with the number of reports on these materials growing from about 5 per year in the early 1990s to about 25 per year in the early 2000s and exceeding 60 in 2009.[8] The structure of APCNs is unique, combining the characteristics of hydrogels and surfactants. Thus, these materials can swell in water but also in organic solvents. Furthermore, when the two types of units are arranged separately in long enough segments, APCNs can phase separate on the nanoscale in selective solvents, just as surfactants and block copolymers. APCNs have been used in a number of applications, most notably as matrices for drug delivery,[9] scaffolds for tissue engineering,[10,11] and membranes for bioartificial pancreas,[12] but also as soft contact lenses,[13] pervaporation membranes,[14] substrates for the growth of Pt nanocrystals,[15] and supports for organic[16] or enzymatic[17] catalysis.

Recent studies on APCNs have involved the preparation of materials with increased structural control, and, in particular, with well-defined one of the two types of segments, either the hydrophobic[18] or the hydrophilic.[19] In an effort to prepare APCNs of better-controlled structure, our research team has been synthesizing for the past 10 years amphiphilic ABA triblock copolymers which were *in situ* end-linked to APCNs.[20] Most of the syntheses were accomplished using group transfer polymerization (GTP),[21] but recent efforts included the use of reversible addition−fragmentation chain transfer (RAFT) polymerization,[22] and atom transfer radical polymerization (ATRP).[23] Several hydrophilic monomers were incorporated, including neutral,[24−26] positively ionizable,[25−41] and negatively ionizable.[42−44] Various hydrophobic monomers were employed too, among which were aliphatic[24−29,31−44] and aromatic ones.[24,30,31] An important type of hydrophobic monomer repeating units, which sometimes are also lipophobic, are semifluorinated monomers. Important properties of fluorine-containing polymers include high thermal and chemical stability, biocompatibility, low surface energy, water nonwettability, and low inflammability. APCNs with fluorine-containing hydrophobic segments have recently been reported, and consisted of a well-defined semifluorinated linear macro-cross-linker, randomly copolymerized either with a hydrophilic monomer[45] or with a hydrophilic macro-cross-linker;[46] in a third example, APCNs based on a fluorinated aromatic hyperbranched core, interconnected with hydrophilic polymers, were prepared.[47]

However, to the best of our knowledge, APCNs based on end-linked ABA triblock copolymers, with semifluorinated mid- or end-blocks, are yet to be reported. Such materials would presumably have a better-controlled structure than the above-mentioned fluoropolymer-containing APCNs. The preparation and characterization

*Author to whom correspondence should be addressed. E-mail: costasp@ucy.ac.cy.

Published on Web 05/25/2010

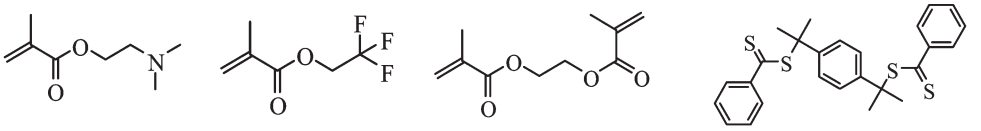

2-(dimethylamino)ethyl methacrylate (DMAEMA): **hydrophilic monomer**

2,2,2-trifluoroethyl methacrylate (TFEMA): **hydrophobic monomer**

ethylene glycol dimethacrylate (EGDMA): **cross-linker**

1,4-bis[2-(thiobenzoylthio) prop-2-yl]benzene (1,4-BTBTPB): **bifunctional CTA**

Figure 1. Chemical structures and names of the main reagents used for the conetwork synthesis.

of these well-defined, semifluorinated APCNs is the aim of the present study. Because of the labile methylene protons next to the fluorinated section, semifluorinated methacrylates may not be polymerized to full monomer conversion via GTP, our synthetic workhorse.[48] Thus, in this work, we decided to employ RAFT polymerization instead, which does not present this problem, and would also allow for the preparation of polymers with molecular weights (MW) higher than those afforded by GTP. Several APCNs were synthesized in this study, in which polymer composition and architecture were systematically varied. The resulting APCNs were thoroughly characterized in terms of their aqueous swelling behavior, and also in terms of their structural organization in water using small-angle neutron scattering (SANS).

Experimental Section

Materials. The monomers, 2,2,2-trifluoroethyl methacrylate (TFEMA, 99%) and 2-(dimethylamino)ethyl methacrylate (DMAEMA, 99%), the cross-linker, ethylene glycol dimethacrylate (EGDMA, 98%), basic alumina, calcium hydride (CaH_2, 90−95%), 2,2-diphenyl-1-picrylhydrazyl hydrate (DPPH, 95%), magnesium, and silica gel (60 Å, 70−230 mesh) were purchased from Aldrich, Germany. *n*-Hexane (≥96%), diethyl ether (≥99.7%), and 1,4-dioxane (99%) were also purchased from Aldrich, Germany. Bromobenzene (≥99.5%) was purchased from Fluka, Germany. 1,4-Diisopropenylbenzene (97%) was purchased from TCI Europe, Belgium. 2,2′-Azobis(isobutyronitrile) (AIBN, 95%), carbon disulfide (purity ≥99.5%), ethanol (99.9%) and deuterated chloroform ($CDCl_3$) were purchased from Merck, Germany. Tetrahydrofuran (THF, 99.8%, both HPLC and reagent grade) was purchased from Scharlau, Spain.

Methods. The DMAEMA monomer and the EGDMA cross-linker were passed through basic alumina columns to remove the inhibitor and any other acidic impurities. They were subsequently stirred over CaH_2 in the presence of the free radical inhibitor DPPH, and were finally freshly distilled prior to use. The TFEMA monomer was simply vacuum-distilled prior to use. The AIBN radical initiator was recrystallized from ethanol. The polymerization solvent 1,4-dioxane was dried over CaH_2 and distilled prior to use. The bifunctional chain transfer agent (CTA) 1,4-bis[2-(thiobenzoylthio)prop-2-yl]benzene (1,4-BTBTPB) was prepared in analogy to the synthesis of 1,3-bis-[2-(thiobenzoylthio)prop-2-yl]benzene as described by Patton et al.[49] In particular, dithiobenzoic acid (DTBA) was reacted with 1,4-diisopropenyl benzene in the presence of a catalytic amount of *p*-toluenesulfonic acid. DTBA was prepared as described by Jayalakshmi et al.[50] Figure 1 displays the chemical structures and the names of the monomers, the cross-linker, and the bifunctional CTA used for the polymer synthesis.

Conetwork Synthesis/Polymerizations. All the conetworks were synthesized by a one-pot, sequential RAFT polymerization. The loading of the EGDMA cross-linker was 6 times the number of moles of the CTA, as determined in the present study in which the synthesis of end-linked DMAEMA homopolymer networks was optimized. Conetworks of different compositions were prepared by varying the polyTFEMA end-block lengths at a constant polyDMAEMA midblock length, whereas conetworks of different architectures were attained by varying the order of addition of the reagents. In particular, ABA and BAB triblock copolymer-based end-linked APCNs were obtained by the sequential addition of the monomers (in the appropriate order) and the cross-linker, while the statistical copolymer-based end-linked conetwork was prepared by the simultaneous copolymerization of the two comonomers, followed by the addition of the cross-linker. Finally, the randomly cross-linked APCN of the statistical copolymer was obtained by the simultaneous terpolymerization of the two comonomers (equimolar) and the cross-linker.

A typical synthetic procedure followed for the synthesis of the equimolar ABA triblock copolymer-based end-linked conetwork $EGDMA_3$-*grad*-$TFEMA_{25}$-*grad*-$DMAEMA_{50}$-*grad*-$TFEMA_{25}$-*grad*-$EGDMA_3$ is described in detail below. A mixture of 83.0 mg of the bifunctional CTA 1,4-BTBTPB (0.178 mmol), 18.3 mg of AIBN (0.112 mmol), 1.50 mL of freshly distilled DMAEMA (1.40 g, 8.90 mmol), and 1.50 mL of 1,4-dioxane were added to a 25 mL Schlenk tube fitted with a magnetic stirring bar. The system was degassed by three freeze−vacuum−thaw cycles, was placed under an inert nitrogen atmosphere, and was heated in an oil bath at 70 °C for 12 h. Subsequently, a sample of the resulting DMAEMA homopolymer was extracted for gel permeation chromatography (GPC) and ^{1}H NMR spectroscopic analyses. Then, 1.30 mL of freshly distilled TFEMA (1.50 g, 8.90 mmol) was added and was left to polymerize for 12 h. After extraction of a sample of the resulting ABA triblock copolymer for analyses, 0.200 mL of the EGDMA cross-linker (0.210 g, 1.06 mmol) was added, leading to the gelation of the solution within 24 h. The BAB triblock copolymer-based end-linked conetwork (with a TFEMA midblock) was obtained using a similar procedure in which the order of addition of the two comonomers was reversed, whereas the statistical copolymer-based end-linked conetwork was synthesized by the simultaneous addition of the two comonomers. The randomly cross-linked conetwork based on statistical copolymers was prepared by the simultaneous addition of the two comonomers and the cross-linker.

Kinetic Study of RAFT Homopolymerization. The homopolymerization by RAFT of the DMAEMA and the TFEMA monomers using the bifunctional CTA 1,4-BTBTPB in the presence of 1,4-dioxane as solvent was followed kinetically for 22 h. The targeted DPs for the DMAEMA and the TFEMA monomers were 50 and 100, respectively. The monomer concentration was 3 M while the AIBN:CTA molar ratio was kept at 0.625:1. Samples were withdrawn at different reaction times and were analyzed by ^{1}H NMR spectroscopy and GPC. In particular, the monomer-to-polymer conversion was determined by ^{1}H NMR spectroscopy, whereas the polymer MWs and the polydispersity indices (PDIs) were characterized by GPC.

Characterization of the Linear Precursors by GPC and ^{1}H NMR Spectroscopy. Linear homopolymer and copolymer samples were obtained before cross-linking and were characterized in terms of their MWs (the number-average MW, M_n, the weight-average MW, M_w, and the PDI = M_w/M_n) and composition using GPC and ^{1}H NMR spectroscopy, respectively. GPC was performed on a Polymer Laboratories system equipped with a Waters 515 isocratic pump, an ERC−7515A Polymer Laboratories refractive index detector and a PL Mixed "D" column. The eluent was THF, pumped at 1 mL min^{-1}. The calibration of the instrument was performed using poly(methyl

methacrylate) (PMMA) standards also supplied by Polymer Laboratories. The ^{1}H NMR spectra of polymer solutions in deuterated chloroform ($CDCl_3$) were recorded using a 300 MHz Avance Bruker NMR spectrometer equipped with an Ultrashield magnet. The copolymer composition was calculated from the ratio of the area of the peak due to the two oxymethylene protons in polyDMAEMA at 4.1 ppm divided by the area of the peak due to the two oxymethylene protons of polyTFEMA at 4.3 ppm. Furthermore, the percentage of unreacted monomers (DMAEMA and TFEMA) was calculated as the ratio of the area of the peak due to the olefinic proton at 5.0 ppm for DMAEMA or 5.2 ppm for TFEMA, divided by the area of the oxymethylene protons of polyDMAEMA (4.1 ppm) or polyTFEMA (4.3 ppm), respectively.

Characterization of the Conetworks. *Determination of the Sol Fraction* (*Extractables*). A small piece from each (co)network was taken immediately after (co)network formation and was promptly characterized in terms of its sol fraction (extractables). These extractables were called "early" extractables. The "early" extractables were obtained by placing the small piece of the conetwork in a small volume of $CDCl_3$ overnight and immediately characterizing the extracted material in terms of its composition by ^{1}H NMR to calculate the final monomer and cross-linker conversions as described previously. The EGDMA conversion was calculated based on the olefinic proton at 6.1 ppm.

Subsequently, the remaining larger piece of each conetwork was taken out of the polymerization Schlenk and was transferred in a 1 L glass jar, where it was left to equilibrate in THF for 2 weeks to remove all the extractables. Afterward, the solution of the extractables was recovered by filtration and the solvent was evaporated off using a rotary evaporator. Then, the thus-predried extractables were further dried under vacuum at room temperature in a vacuum oven for 72 h. The sol fraction was calculated as the ratio of the dried mass of the extracted polymer to the theoretical mass of the conetwork estimated as the sum of the masses of the CTA, the monomers, and the cross-linker. The extractables were also characterized using GPC and ^{1}H NMR spectroscopy.

Measurement of the Degree of Swelling (*DS*). All (co)networks were characterized in terms of their degrees of swelling (DSs) in THF and in aqueous solutions covering the pH range between 1.5 to 12. The THF-equilibrated (co)networks were cut in small pieces and were weighed to determine their THF-swollen mass. Subsequently, the (co)network pieces were dried in a vacuum oven (at room temperature) for 3 days, and their dry mass was determined. The DSs were calculated as the ratios of the swollen divided by the dried (co)network masses. The characterization of the aqueous DSs at different pHs was performed by transferring the dried (co)networks in a volume of water where the appropriate volume of a 0.5 M HCl standard solution had been added so that a desired degree of ionization of the DMAEMA units was attained. The number of moles of HCl required for each sample was calculated by multiplying the desired degree of ionization times the number of moles of DMAEMA units present in each sample. The latter was calculated as the conetwork dry mass times the percentage of DMAEMA units in the conetwork divided by the MW of the DMAEMA unit. In addition to the acidified (co)network samples, three more samples were prepared for each different (co)network. Of these three samples, two were made alkaline by the addition of small volumes of a 0.5 M NaOH standard solution, while the third sample remained neutral (without the addition of acid or base). The samples were equilibrated for 3 weeks and the swollen masses were measured. The DSs of the samples were again calculated by dividing the swollen mass by the dry mass of each (co)network sample.

Small-Angle Neutron Scattering (*SANS*). All the (co)networks of this study were characterized using SANS. Dried (co)network samples, in the uncharged state, were placed in D_2O where they were allowed to equilibrate. SANS measurements were performed on the 30 m NG7 instrument at the Center for Neutron Research of the National Institute of Standards and Technology (NIST) in Gaithersburg, Maryland. The incident wavelength λ was 6 Å. Three sample-to-detector distances, 1.00, 4.00, and 13.50 m, were employed, covering a q-range [$q = (4\pi/\lambda)\sin(\theta/2)$] from 0.034 to 5.600 nm^{-1}. The samples were loaded in quartz cells of 1 mm thickness. The scattering patterns were isotropic, and therefore, the measured counts were circularly averaged. The averaged data were corrected for empty cell and background. The distance between the scattering centers was estimated from the position of the intensity maximum q_{max}, as $2\pi/q_{max}$.

Results and Discussion

Controlled Polymerization of Semifluorinated Monomer. Central to our syntheses was the controlled polymerization of the TFEMA monomer. To date, there is only one report describing the controlled RAFT polymerization of this monomer, yielding block, gradient, and random copolymers.[51] However, the kinetics of TFEMA RAFT polymerization was not reported in that previous study, which is a task also undertaken in the present investigation, and described in the following paragraph.

Kinetics of DMAEMA and TFEMA RAFT Homopolymerizations. The kinetics of homopolymerization of TFEMA and DMAEMA was studied by determining the monomer conversion and the polymer M_n and PDI for the samples extracted at various reaction times. Figure 2 presents the collected kinetic data in different plots. In particular, Figure 2a shows the temporal evolution of the conversion (determined by ^{1}H NMR spectroscopy) of the two monomers, Parts b and c of Figure 2 display the time-dependence of M_n and PDI, respectively, Figure 2d plots M_n against monomer conversion, and Figure 2e is the first-order kinetic plot for monomer conversion, x. Figure 2a reveals that the homopolymerization of DMAEMA has an induction period of about 20 min, while that of TFEMA has an induction time of 60 min. Figure 2b shows how the M_n values of the two homopolymers increase with time, while Figure 2c shows that the PDIs also increase with time and reach the value of 1.6 for the homopolymerization of DMAEMA and of 1.5 for the homopolymerization of TFEMA. The variation of M_n with monomer conversion (Figure 2d) for both the DMAEMA and the TFEMA homopolymerizations was linear, indicating the "living" character of the polymerizations. The plots of $\ln(1/(1 - x))$ vs time (Figure 2e), where x is the monomer conversion, were linear for both monomers, indicating that the polymerizations followed first-order kinetics. The rate constants for the homopolymerization reactions calculated from Figure 2e were 6.44×10^{-2} M^{-1} min^{-1} for DMAEMA and 6.72×10^{-2} M^{-1} min^{-1} for TFEMA, indicating that the homopolymerization of TFEMA was slightly faster than that of DMAEMA.

Synthesis of End-Linked Semifluorinated Amphiphilic Conetworks. Six semifluorinated APCNs and two end-linked homopolymer networks were synthesized by sequential RAFT polymerization, using AIBN as the initiator, 1,4-BTBTPB as the CTA, 1,4-dioxane as the solvent, and DMAEMA and TFEMA as the (co)monomers. The synthetic procedure for the preparation of the end-linked APCNs is illustrated schematically in Figure 3, where the synthesis of the end-linked conetwork based on the TFEMA$_{25}$-*grad*-DMAEMA$_{50}$-*grad*-TFEMA$_{25}$ (gradient) triblock copolymer is presented. The DMAEMA units are colored in light blue while the TFEMA units are painted dark green. The black circles in the conetwork represent the EGDMA cores. The synthesis involved sequential rather than stepwise monomer and cross-linker additions to enhance the livingness of the polymerization and enable conetwork formation. In preliminary

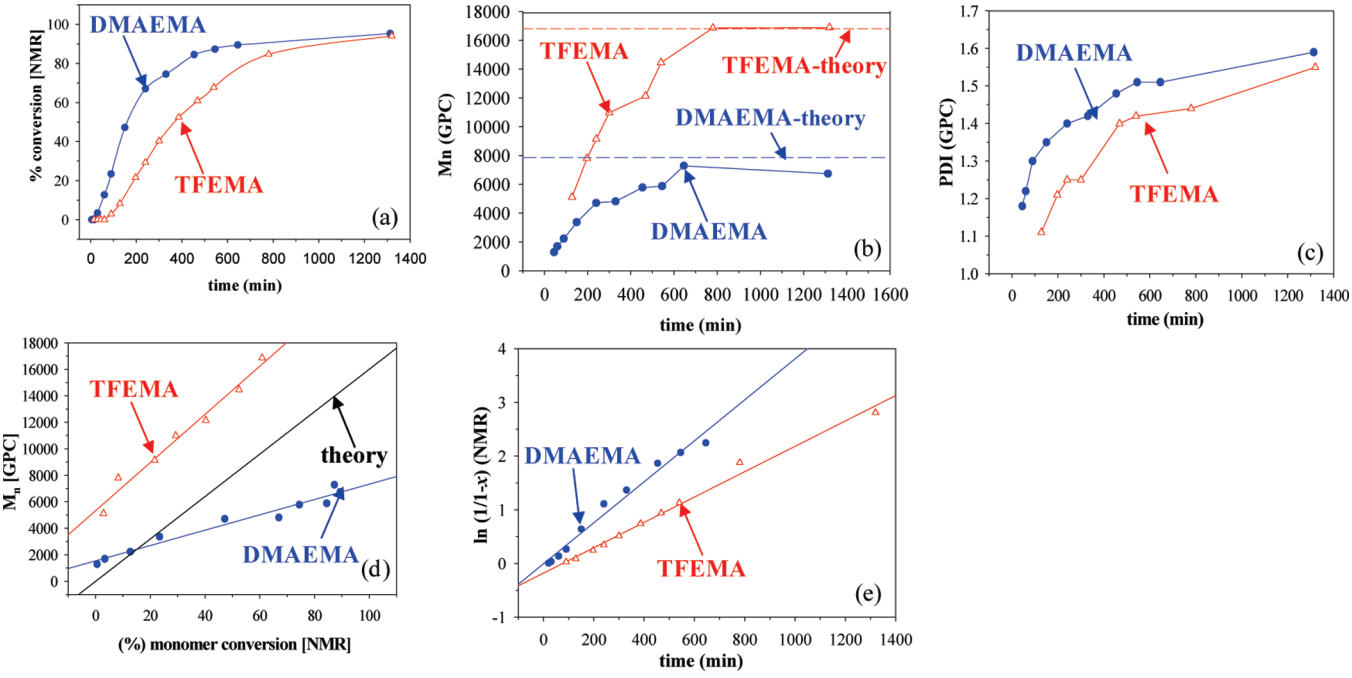

Figure 2. Temporal evolution of (a) monomer (DMAEMA and TFEMA) conversion, (b) number-average molecular weight, M_n, and (c) polydispersity index, PDI, (d) dependence of M_n on monomer conversion, and (e) first-order kinetic plots for the conversion of the two monomers. Targeted DP = 50 for DMAEMA and DP = 100 for TFEMA; monomer concentration = 3 M, [AIBN]:[CTA] = 0.625:1.

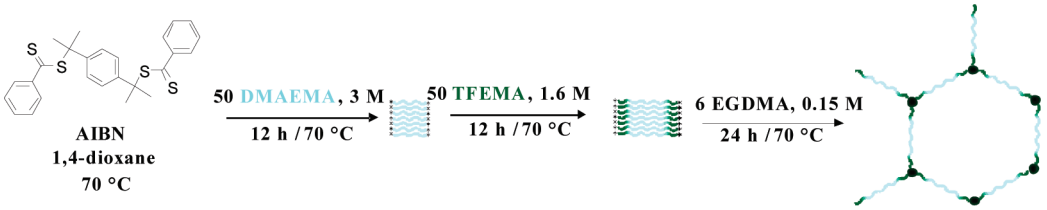

Figure 3. Schematic representation of the synthetic procedure followed for the preparation of the end-linked conetwork based on the triblock copolymer TFEMA$_{25}$-*grad*-DMAEMA$_{50}$-*grad*-TFEMA$_{25}$. The DMAEMA units are shown in light blue, while the TFEMA units are painted dark green. Black circles represent EGDMA cross-linker cores.

experiments, the synthesis was attempted using stepwise additions, where the reaction was stopped and the polymer was recovered and isolated. However, in those experiments, a higher loading of cross-linker was necessary to effect gelation; a 6:1 EGDMA: CTA molar ratio was not sufficient to effect conetwork formation in those experiments.

Figure 3 shows that the first step resulted in the preparation of the linear DMAEMA homopolymer with both active ends (indicated by asterisks) due to the use of the bifunctional CTA. The second step involved the addition of TFEMA to induce chain growth and synthesis of the TFEMA-*grad*-DMAEMA-*grad*-TFEMA triblock copolymer with two active ends. Finally, the addition of the cross-linker resulted in the formation of a three-dimensional conetwork via the interconnection of the active polymer chain ends. In all cases, the polymerization system remained homogeneous and no immiscibility was observed.

The 6:1 molar ratio of cross-linker to CTA used was determined in this study as the optimum loading for sufficient incorporation of chains in to end-linked DMAEMA homopolymer networks. Table 1 shows the monomer and cross-linker conversions, the MWs and the PDIs of the linear DMAEMA homopolymer precursors to the homopolymer networks as measured by ^{1}H NMR spectroscopy and GPC. The gelation time for network formation is also shown in the table.

Table 2 shows the monomer and cross-linker conversions, and the polymer MWs, PDIs, and compositions for all homopolymer and copolymer end-linked (co)networks synthesized at the optimum 6:1 cross-linker:CTA molar ratio. We prepared three end-linked APCNs based on ABA triblock copolymers with DMAEMA midblocks, one end-linked APCN based on a BAB triblock copolymer with a TFEMA midblock, one end-linked APCN based on a statistical copolymer, and, finally, one randomly cross-linked statistical APCN. The two end-linked homopolymer networks, one for each of the two monomers, were synthesized too.

Molecular Weights and Composition of the Precursors. Figure 4 shows the GPC traces of the precursors to all the (co)networks. The chromatograms show that the MWs of the triblock copolymers were greater than those of the corresponding homopolymers, as expected. Table 2 shows the monomer conversion determined by GPC and ^{1}H NMR spectroscopy and the MWs and compositions of the linear precursors to the conetworks as measured by GPC and ^{1}H NMR spectroscopy, respectively. The monomer and the cross-linker conversions were determined from the "early" extractables. The DMAEMA monomer conversions determined by ^{1}H NMR spectroscopy ranged between 85.7 and 98% for conetworks with a DMAEMA middle-block, and it was 58.8% for the conetwork with DMAEMA end-blocks. The conversions of TFEMA for all (co)networks were

Table 1. Monomer Conversion, Molecular Weights, Polydispersity Indices, and Gelation Times of the End-Linked DMAEMA Homopolymer Networks, Prepared for the Optimization of the Cross-Linker Loading

		% conversion of DMAEMA[a]		GPC results				
no.	CTA:EGDMA[a]	GPC	^{1}H NMR	M_n	M_w/M_n	DP	EGDMA conversion	gelation time (h)
1	1:2	75.4	75.6	11 700	1.6	72	80.9	no gel
2	1:4	94.3	93.9	16 900	1.6	105	93.0	8−24
3	1:6	94.2	91.7	16 000	1.5	99	93.4	3.5
4	1:8	81.0	83.0	15 900	1.4	98	97.4	3.3

[a] DMAEMA: 2-(dimethylamino)ethyl methacrylate. EGDMA: ethylene glycol dimethacrylate.

Table 2. Monomer and Cross-Linker Conversions, Molecular Weights, Polydispersity Indices, and Compositions of the Linear Homopolymer and Copolymer Precursors to the (Co)Networks As Measured by GPC and ^{1}H NMR Spectroscopy

		conversion (mol %)[b]						GPC results		% mol TF	
no.	polymer structure[a]	TF	D	E	time (min)	gelation time (min)	MW_{theor}[c]	M_n	M_w/M_n	theor	^{1}H NMR
1	D_{100}		85.7		710	180	16 000	15 300	1.50	0	0
	E_3-*grad*-D_{100}-*grad*-E_3		91.7	81.7	1440						
2	TF_{100}	99.0			780	180	17 000	16 900	1.45	100	100
	E_3-*grad*-TF_{100}-*grad*-E_3	99.2		99.8	1440						
3	D_{50}		94.0		605	435	8000	9530	1.62	0	0
	$TF_{12.5}$-*grad*-D_{50}-*grad*-$TF_{12.5}$	85.0	100		740		12 500	12 500	1.66	33.3	22.5
	E_3-*grad*-$TF_{12.5}$-*grad*-D_{50}-*grad*-$TF_{12.5}$-*grad*-E_3	99.3	100	98.1	1440						
4	D_{50}		95.8		710	≤540	8000	8120	1.50	0	0
	TF_{25}-*grad*-D_{50}-*grad*-TF_{25}	79.0	100		710		17 000	20 800	1.51	50.0	49.5
	E_3-*grad*-TF_{25}-*grad*-D_{50}-*grad*-TF_{25}-*grad*-E_3	99.1	100	97.5	1440						
5	TF_{50}	77.3			729	≤540	9000	9000	1.47	100	100
	D_{25}-*grad*-TF_{50}-*grad*-D_{25}	91.2	58.8		696		17 000	11 600	1.70	50.0	55.2
	E_3-*grad*-D_{25}-*grad*-TF_{50}-*grad*-D_{25}-*grad*-E_3	98.3	96.5	94.3	1440						
6	D_{50}		87.2		625	≤540	8000	9630	1.59	0	0
	$TF_{37.5}$-*grad*-D_{50}-*grad*-$TF_{37.5}$	81.5	99.1		695		21 000	20 400	1.81	60.0	58.6
	E_3-*grad*-$TF_{37.5}$-*grad*-D_{50}-*grad*-$TF_{37.5}$-*grad*-E_3	93.6	100	83.5	1440						
7	D_{50}-*co*-TF_{50}	98.5	98.0		625	≤425	17 000	14 700	1.46	50.0	48.5
	E_3-*grad*-(D_{50}-*co*-TF_{50})-*grad*-E_3	99.5	99.5	99.5	1440						
8	D_{50}-*co*-TF_{50}-*co*-E_6	99.5	99.5	99.5	1440	130−610					

[a] D: 2-(dimethylamino)ethyl methacrylate. TF: 2,2,2-trifluoroethyl methacrylate. E: ethylene glycol dimethacrylate. [b] From "early" extractables. [c] $MW_{theor.} = [M]/[CTA] \times (\text{monomer conversion}) \times MW_{monomer} + MW_{CTA}$

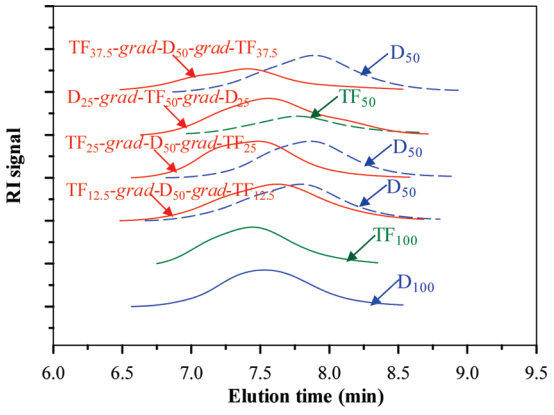

Figure 4. GPC eluograms of the homopolymer and the triblock copolymer precursors to all the (co)networks.

between 77 and 100%. The DMAEMA and TFEMA conversions determined using either ^{1}H NMR spectroscopy or GPC were very similar. The M_n values were found to be very close to those expected on the basis of the monomer to CTA ratio. Table 2 also shows the EGDMA conversion for all the (co)networks. In all cases, the EGDMA conversions were higher than 81% but in no case did they reach full conversion possibly due to steric hindrances.

The successful formation of the linear homopolymer and copolymer precursors to the (co)networks was also confirmed by ^{1}H NMR spectroscopy. Figure 5a shows the ^{1}H NMR spectrum of the $DMAEMA_{50}$ homopolymer, with the peaks at 5.5 and 6.1 ppm corresponding to the olefinic protons of some unreacted monomer, whereas Figure 5b presents the ^{1}H NMR spectrum of $TFEMA_{25}$-*grad*-$DMAEMA_{50}$-*grad*-$TFEMA_{25}$. In the latter spectrum, in addition to the polymer peaks (e.g., proton f), there were also monomer peaks (e.g., proton i, indicating that the conversion of TFEMA was not complete.

Sol Fraction. The results of the characterization of the extractables are listed in Table 3, including their percentage, M_n, and PDI. The percentage of the extractables (sol fraction) varied from 2.8 to 21.0%, with the highest percentage corresponding to the conetwork with the longest polyTFEMA block (with a DP equal to 75). The relatively low percentages of the extractables indicate the successful incorporation of the linear precursors into the (co)network. In the case of $EGDMA_3$-*grad*-$TFEMA_{37.5}$-*grad*-$DMAEMA_{50}$-*grad*-$TFEMA_{37.5}$-*grad*-$EGDMA_3$ end-linked triblock copolymer-based conetwork, the high percentage of extractables can be attributed to the long copolymer precursor which could not be effectively incorporated in to the conetwork. The extractables mainly consisted of linear chains (polyDMAEMA, polyTFEMA, or poly(DMAEMA-*grad*-TFEMA)) which were probably terminated before the addition of the cross-linker. The composition of the extractables in polyDMAEMA was higher in the cases when DMAEMA was used as the first monomer, as the polyDMAEMA midblock was subjected to deactivation longer than its daughter ABA triblock copolymer. The M_n of the main peak of the extractables shown also in Table 3 was comparable to those of the corresponding linear precursors (Table 1).

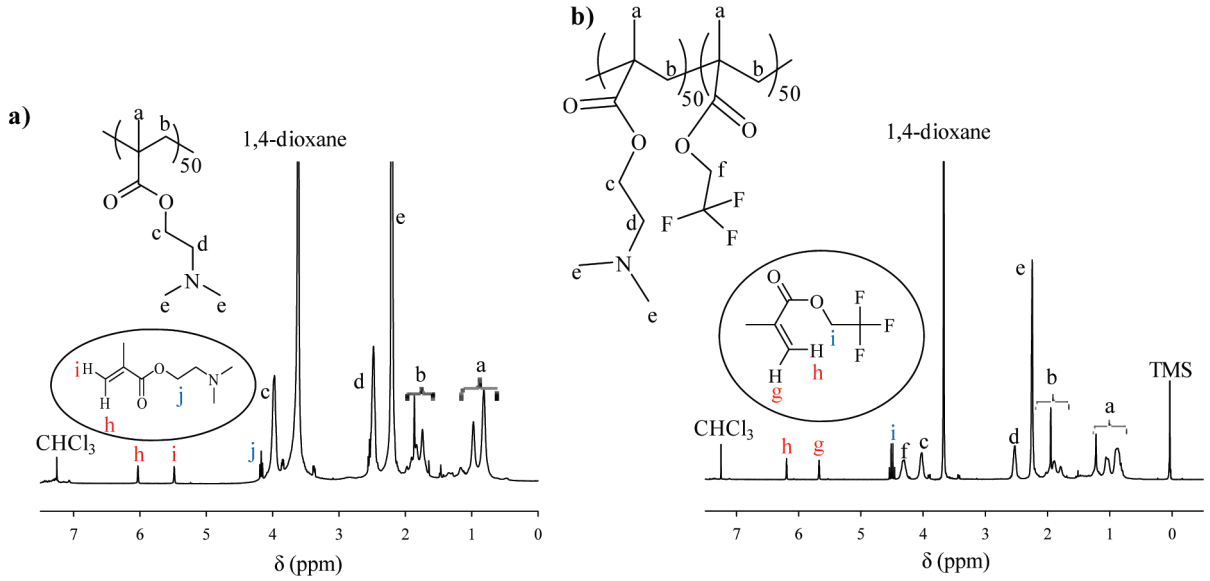

Figure 5. ^{1}H NMR spectra of (a) the $DMAEMA_{50}$ homopolymer and (b) the $TFEMA_{25}$-*grad*-$DMAEMA_{50}$-*grad*-$TFEMA_{25}$ triblock copolymer.

Table 3. Percentage, Compositions, and Molecular Weights of the Extractables from the (Co)Networks

			% composition of extractables (^{1}H NMR)					GPC results	
a/a	network structure[a]	extractables %	PD	PTF	D	TF	E	M_n	PDI
1	E_3-*grad*-D_{100}-*grad*-E_3	10.5	99.6				0.4	6410	1.7
								134	1.0
2	E_3-*grad*-TF_{100}-*grad*-E_3	8.7		100				17 600	1.7
								459	1.1
3	E_3-*grad*-$TF_{12.5}$-*grad*-D_{50}-*grad*-$TF_{12.5}$-*grad*-E_3	5.7	69.9	18.5			11.6	11 000	1.8
								197	1.1
4	E_3-*grad*-TF_{25}-*grad*-D_{50}-*grad*-TF_{25}-*grad*-E_3	9.0	62.1	36.0			1.9	12 700	1.7
								300	1.1
5	E_3-*grad*-D_{25}-*grad*-TF_{50}-*grad*-D_{25}-*grad*-E_3	7.6	36.8	49.7	5.8		7.7	19 600	2.4
								260	1.0
6	E_3-*grad*-$TF_{37.5}$-*grad*-D_{50}-*grad*-$TF_{37.5}$-*grad*-E_3	21.0	49.7	47.3		0.7	2.3	19 300	5.4
								108	1.0
7	E_3-*grad*-(D_{50}-*co*-TF_{50})-*grad*-E_3	5.9	52.1	47.7			0.2	19 900	1.5
8	D_{50}-*co*-TF_{50}-*co*-E_6	2.8	32.1	49.4		18.5			

[a] D: 2-(dimethylamino)ethyl methacrylate. TF: 2,2,2-trifluoroethyl methacrylate. E: ethylene glycol dimethacrylate.

Degrees of Swelling and Ionization of the Networks. The experimentally measured DSs and degrees of ionization of all the (co)networks are plotted against pH in Figure 6. The theoretical structure of each (co)network is indicated above each plot. A general feature of these plots is that each DS vs pH curve followed the corresponding degree of ionization vs pH curve, confirming the importance of charge on (co)network swelling. The (co)networks began to swell below pH 7 because of the presence of the units of DMAEMA, a tertiary amine becoming ionized mainly in the acidic pH range (pH $\leq$ 8).[52,53] The ionization of the DMAEMA units resulted in electrostatic repulsions between the positively charged chains, and in the buildup of an osmotic pressure created by the counterions to the charges in the (co)networks.[54,55] The DSs presented a maximum at pH $\sim$ 3.0−4.5, followed by a decrease at lower pH values (pH $\sim$ 2), probably due to the increase in ionic strength effected by the relatively high concentration of HCl under these conditions. The plots in Figure 6 were used to extract the effective p*K*s and the aqueous DSs at low and neutral pH of the (co)networks, which are presented in the following sections.

Effective p*K*s of the (Co)networks. The effective p*K* values of the DMAEMA units in the (co)networks were read out from the degree of ionization vs pH curves as the pH at 50% ionization and are presented in Table 4. The p*K* values decreased slightly as the TFEMA content increased. This is in agreement with previous studies by our Group on APCNs.[25−41] The increase in the TFEMA content leads to an increase in hydrophobicity, a reduction of the local dielectric constant, and a strengthening of the Coulombic interactions, which render conetwork ionization more difficult.[54] The p*K*s span a range of values from 3.9 to 5.3 which are lower than that of the DMAEMA homopolymer-based network (pK = 7), as was shown previously by our Group.[25−41] The latter was also lower than that of the DMAEMA monomer which is approximately 8.5.

Degrees of Swelling in Water and in THF. The aqueous DSs at pH $\sim$ 7 and at pH 2 as well as the DSs in THF for all the (co)networks are listed in Table 4 and are plotted in Figure 7. Figure 7a presents the effect of polymer composition while Figure 7b presents the effect of polymer architecture. Figure 7a shows that the DSs in pure and in acidified water decreased as the content in TFEMA increased. In particular, the DSs in low pH water decreased from about 11.1 down to 2.3 as the DP of the TFEMA blocks increased from 25 to 75. These DSs were higher as compared to those in pure water and in THF because of the full ionization of the DMAEMA units at low pH. The DSs of the conetworks in THF also decreased with the increase in the TFEMA content. This behavior may indicate a greater affinity of the

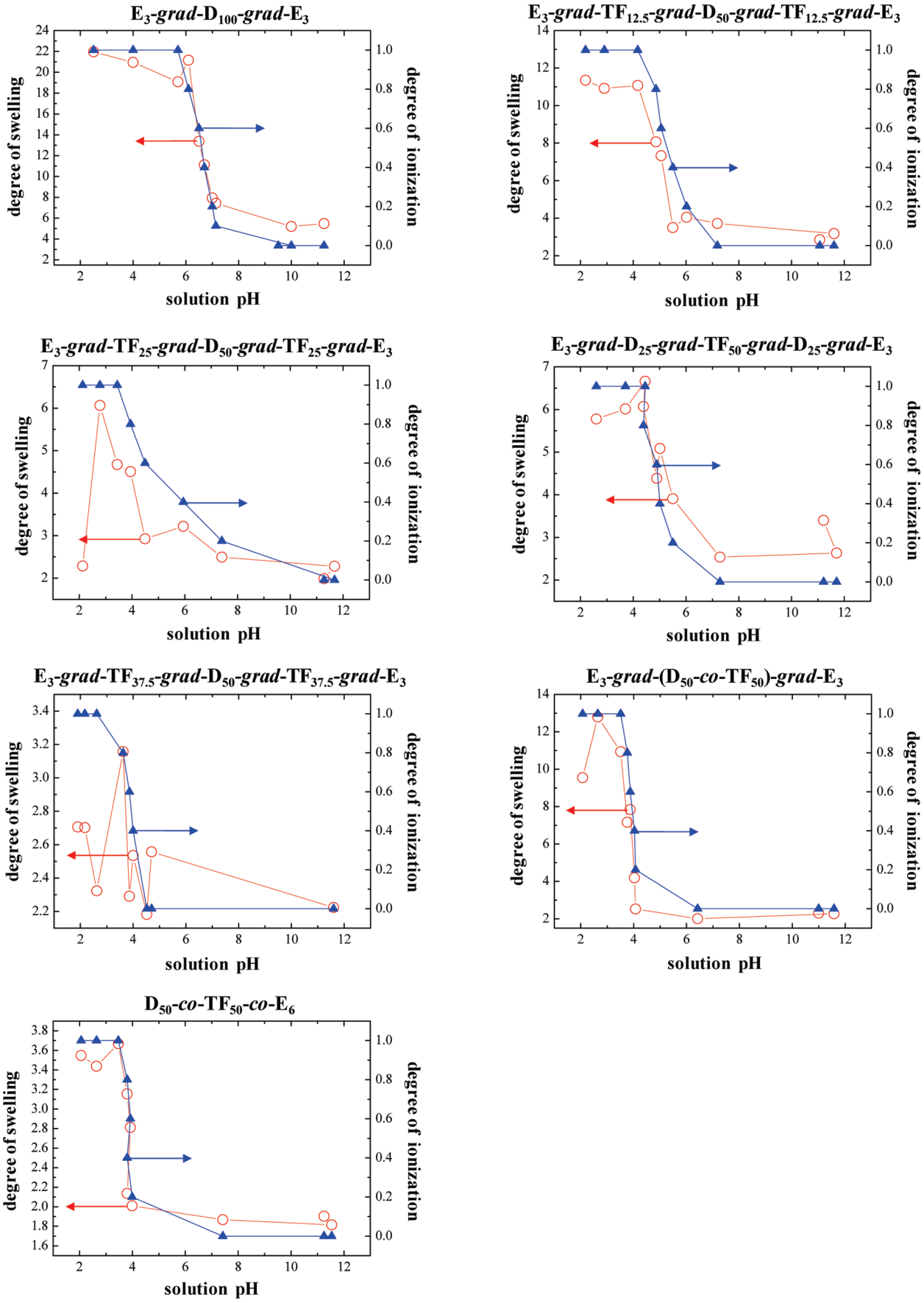

Figure 6. Degrees of swelling and degrees of ionization as a function of pH for all the (co)networks.

Table 4. Degrees of Swelling in THF and in Pure and Acidic Water, and Effective p*K*s of the DMAEMA Monomer Repeating Units of all the (Co)Networks

a/a	network structure[a]	degree of swelling			effective p*K*
		THF	pure water	acidic water	
1	E_3-*grad*-D_{100}-*grad*-E_3	6.3 ± 0.2	5.2 ± 1.6	22.0 ± 1.6	7.0
2	E_3-*grad*-TF_{100}-*grad*-E_3	6.4 ± 0.5	2.3 ± 0.3		
3	E_3-*grad*-$TF_{12.5}$-*grad*-D_{50}-*grad*-$TF_{12.5}$-*grad*-E_3	8.9 ± 0.5	3.7 ± 1.3	11.1 ± 2.9	5.3
4	E_3-*grad*-TF_{25}-*grad*-D_{50}-*grad*-TF_{25}-*grad*-E_3	5.3 ± 0.6	2.3 ± 0.5	2.7 ± 1.4	5.0
5	E_3-*grad*-D_{25}-*grad*-TF_{50}-*grad*-D_{25}-*grad*-E_3	11.5 ± 0.6	2.5 ± 0.9	6.7 ± 0.5	5.3
6	E_3-*grad*-$TF_{37.5}$-*grad*-D_{50}-*grad*-$TF_{37.5}$-*grad*-E_3	3.8 ± 0.9	2.6 ± 0.8	2.3 ± 0.5	3.9
7	E_3-*grad*-(D_{50}-*co*-TF_{50})-*grad*-E_3	4.2 ± 0.4	2.0 ± 0.5	10.9 ± 5.2	4.0
8	D_{50}-*co*-TF_{50}-*co*-E_6	2.6 ± 0.2	1.9 ± 0.3	3.7 ± 0.5	3.9

[a] D: 2-(dimethylamino)ethyl methacrylate. TF: 2,2,2-trifluoroethyl methacrylate. E: ethylene glycol dimethacrylate.

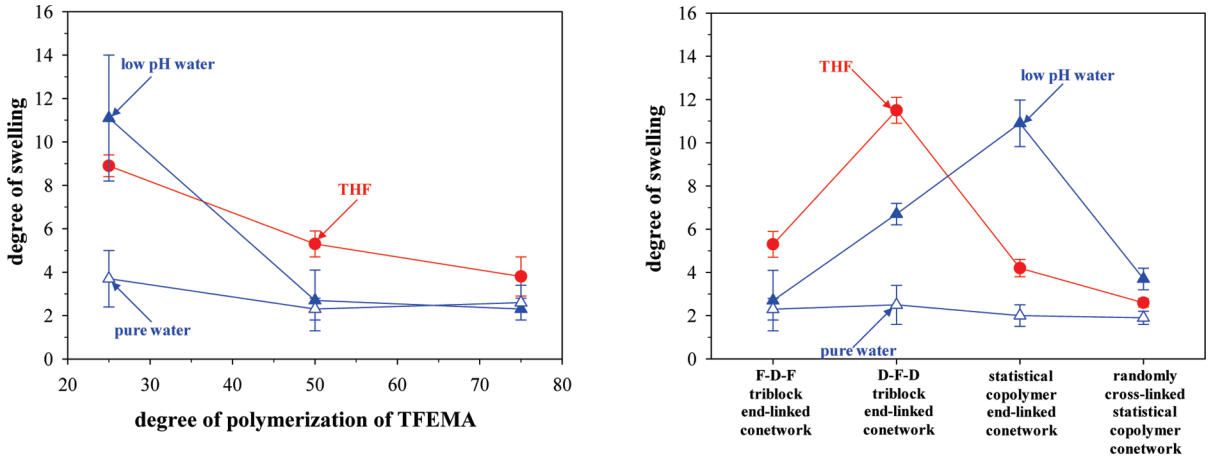

Figure 7. Degrees of swelling of the conetworks in THF, in pure water and in low pH water vs (a) polymer composition and (b) polymer architecture.

DMAEMA units for THF as compared to that of the semifluorinated monomer repeating units for THF.

Figure 7b illustrates the effect of polymer architecture on the DSs. In pure water, all isomeric conetworks were collapsed, exhibiting minimum DSs close to 2. In acidic water, the DS of the TFEMA-*grad*-DMAEMA-*grad*-TFEMA (F−D−F) end-linked triblock copolymer-based conetwork was lower than that of the DMAEMA-*grad*-TFEMA-*grad*-DMAEMA (D−F−D) end-linked triblock copolymer-based conetwork due to the placement of hydrophobic TFEMA block next to the EGDMA cores in the F−D−F conetwork, increasing its hydrophobicity. The THF and low pH aqueous DSs of the randomly cross-linked statistical copolymer conetwork were lower than those of the other isomeric conetworks. This was also observed in previous work by our group[25−41] and was attributed to the broad distribution of the chain lengths between cross-links. The presence of some shorter-than-average chains may dominate the swelling behavior and result in the low DSs observed.

Nanoscale Phase Separation. Figure 8 shows the SANS profiles of all the end-linked semifluorinated APCNs in the uncharged state in D_2O, whereas Table 5 lists the separation distance between the scattering centers, calculated from the position of the scattering peak in the SANS profiles. Figure 8a illustrates the effect of (co)network composition, while Figure 8b presents the effect of conetwork architecture. In Figure 8a, the SANS profiles of the two most hydrophobic end-linked conetworks, $EGDMA_3$-*grad*-$TFEMA_{25}$-*grad*-$DMAEMA_{50}$-*grad*-$TFEMA_{25}$-*grad*-$EGDMA_3$ and $EGDMA_3$-*grad*-$TFEMA_{37.5}$-*grad*-$DMAEMA_{50}$-*grad*-$TFEMA_{37.5}$-*grad*-$EGDMA_3$, exhibited single distinct peaks, whereas that of the less hydrophobic conetwork

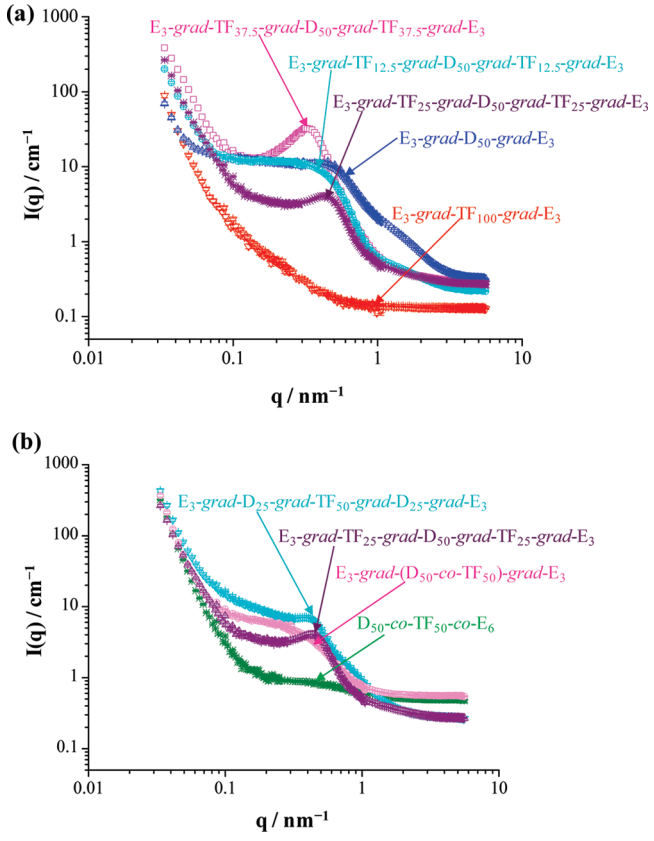

Figure 8. SANS profiles of all the (co)networks in D_2O. (a) Effect of (co)network composition. (b) Effect of conetwork architecture.

Table 5. Spacing between the Scattering Centers, q_{max} Values, and Degrees of Swelling in Pure Water of All of the Conetworks

a/a	network structure[a]	q_{max} (nm^{-1})	d (nm)	$DS_{pure\ water}$
1	E_3-*grad*-D_{50}-*grad*-E_3	no peak		5.2
2	E_3-*grad*-TF_{100}-*grad*-E_3	no peak		2.3
3	E_3-*grad*-$TF_{12.5}$-*grad*-D_{50}-*grad*-$TF_{12.5}$-*grad*-E_3	shoulder		3.7
4	E_3-*grad*-TF_{25}-*grad*-D_{50}-*grad*-TF_{25}-*grad*-E_3	0.452	13.9	2.5
5	E_3-*grad*-D_{25}-*grad*-TF_{50}-*grad*-D_{25}-*grad*-E_3	0.404	15.5	2.5
6	E_3-*grad*-$TF_{37.5}$-*grad*-D_{50}-*grad*-$TF_{37.5}$-*grad*-E_3	0.330	19.0	2.2
7	E_3-*grad*-(D_{50}-*co*-TF_{50})-*grad*-E_3	no peak		2.0
8	D_{50}-*co*-TF_{50}-*co*-E_6	no peak		1.9

[a] D: 2-(dimethylamino)ethyl methacrylate. TF: 2,2,2-trifluoroethyl methacrylate. E: ethylene glycol dimethacrylate.

$EGDMA_3$-*grad*-$TFEMA_{12.5}$-*grad*-$DMAEMA_{50}$-*grad*-$TFEMA_{12.5}$-*grad*-$EGDMA_3$ and that of the hydrophilic DMAEMA homopolymer network $EGDMA_3$-*grad*-$DMAEMA_{50}$-*grad*-$EGDMA_3$ did not display any peak but only a shoulder. Finally, the SANS profile of the TFEMA hydrophobic homopolymer network presented neither a peak nor a shoulder. The presence of the peaks in the two more hydrophobic end-linked triblock copolymer-based conetworks can be attributed to the organization of the semifluorinated hydrophobic blocks in to larger hydrophobic domains, resulting in nanoscale phase separation. The presence of a shoulder in the case of the conetwork $EGDMA_3$-*grad*-$TFEMA_{12.5}$-*grad*-$DMAEMA_{50}$-*grad*-$TFEMA_{12.5}$-*grad*-$EGDMA_3$ can be again attributed to the formation of hydrophobic clusters, which, however, are smaller than the previously mentioned ones due to the shorter hydrophobic blocks. The shoulder in the case of the $DMAEMA_{50}$ homopolymer-based network can be attributed to the scattering by the EGDMA cross-linker nodes. The absence of a peak in the case of the $EGDMA_3$-*grad*-$TFEMA_{100}$-*grad*-$EGDMA_3$ homopolymer-based conetwork was due to the lack of scattering contrast, as this network did not absorb D_2O, a result of its high hydrophobicity. For the two more hydrophobic conetworks, as the PTFEMA content increased, the peak became more discrete while its position was shifted to lower q-values, indicating a more extensive nanoscale phase separation and a larger spacing between the scattering centers, respectively. In particular, the spacing between the scattering centers, calculated as $2\pi/q_{max}$ was found to be 13.9 and 19.0 nm (Table 5) for conetworks 4 and 6, respectively. These spacings should be compared to the contour lengths of 25 and 31 nm of the respective chains, suggesting chain coiling, arising from the limited aqueous swelling of these conetworks and their nanoscale phase separation discussed above.

Figure 8b plots the SANS profiles of the four isomeric end-linked conetworks having different architectures. The profiles of the F−D−F and the D−F−D triblock copolymer-based end-linked conetworks presented single peaks, the end-linked conetwork based on the statistical copolymer presented a shoulder, and the randomly cross-linked conetwork did not present any peak or shoulder. The D−F−D triblock copolymer-based end-linked conetwork presented a slightly greater distance between the scattering centers as compared to the F−D−F triblock copolymer-based end-linked conetwork due to the less efficient nanoscale phase separation in the former conetwork, arising from the placement of the hydrophobic semifluorinated block in the middle of the chain, away from the EGDMA hydrophobic cross-linking cores. The presence of a shoulder in the statistical copolymer-based end-linked conetwork can be attributed to the scattering by the hydrophobic EGDMA cross-linker nodes, while the absence of scattering peaks in the randomly cross-linked copolymer conetwork can be attributed to the random distribution of the hydrophobic units in the chain of these conetworks, which precluded nanophase separation. The latter is in agreement with previous neutron scattering studies on APCNs in D_2O reported by our group.[42,43]

Conclusions

RAFT polymerization was successfully employed for the preparation of six semifluorinated amphiphilic conetworks based on TFEMA and DMAEMA. The extractables from all the conetworks were low, indicating successful conetwork formation. The lowest DSs were obtained in pure water, a selective solvent for the DMAEMA units, intermediate DSs were observed in THF which was a nonselective solvent, and the highest DSs were measured in acidic water which was also a selective solvent for the DMAEMA units which were now completely ionized. As the PTFEMA content increased, SANS indicated that the APCNs were internally organized forming larger semifluorinated hydrophobic domains.

Acknowledgment. We thank the Cyprus Research Promotion Foundation and EU Structural and Cohesion Funds for Cyprus for supporting this work in the form of a PENEK2008 Doctoral Research Grant (Project ENISX/0308/048) to K.S.P. We are also grateful to the A. G. Leventis Foundation for a generous donation that enabled the purchase of the NMR spectrometer of the University of Cyprus, and the National Institute of Standards and Technology and the U.S. Department of Commerce in providing the neutron research facilities used in this work.

References and Notes

(1) Mespouille, L.; Hedrick, J. L.; Dubois, P. *Soft Matter* **2009**, *5*, 4878–4892.
(2) Gitsov, I. *J. Polym. Sci., Part A: Polym. Chem.* **2008**, *46*, 5295–5314.
(3) Erdodi, G.; Kennedy, J. P. *Prog. Polym. Sci.* **2006**, *31*, 1–18.
(4) Patrickios, C. S.; Georgiou, T. K. *Curr. Opin. Colloid Interface Sci.* **2003**, *8*, 76–85.
(5) Weber, M.; Stadler, R. *Polymer* **1988**, *29*, 1064–1070.
(6) Weber, M.; Stadler, R. *Polymer* **1988**, *29*, 1071–1078.
(7) Chen, D.; Kennedy, J. P.; Allen, A. J. *J. Macromol. Sci., Chem.* **1988**, *A25*, 389–401.
(8) Source: Web of Science, searched on March 9, 2010, using keywords "amphiphilc networks or conetworks."
(9) Bromberg, L.; Temchenko, M.; Hatton, T. A. *Langmuir* **2002**, *18*, 4944–4952.
(10) Tanahashi, K.; Jo, S.; Mikos, A. G. *Biomacromolecules* **2002**, *3*, 1030–1037.
(11) Rimmer, S.; Wilshaw, S.-P.; Pickavance, P.; Ingham, E. *Biomaterials* **2009**, *30*, 2468–2478.
(12) Grundfest-Broniatowski, S. F.; Tellioglu, G.; Rosenthal, K. S.; Kang, J.; Erdodi, G.; Yalcin, B.; Cakmak, M.; Drazba, J.; Bennett, A.; Lu, L.; Kennedy, J. P. *ASAIO J.* **2009**, *55*, 400–405.
(13) Nicolson, P. C.; Vogt, J. *Biomaterials* **2001**, *22*, 3273–3283.
(14) Du Prez, F. E.; Goethals, E. J.; Schué, R.; Qariouh, H.; Schué, F. *Polym. Int.* **1998**, *46*, 117–125.
(15) Christodoulakis, K. E.; Palioura, D.; Anastasiadis, S. H.; Vamvakaki, M. *Top. Catal.* **2009**, *52*, 394–411.
(16) Hensle, E. M.; Tobis, J.; Tiller, J. C.; Bannwarth, W. *J. Fluor. Chem.* **2008**, *129*, 968–973.

(17) Savin, G.; Bruns, N.; Thomann, Y.; Tiller, J. C. *Macromolecules* **2005**, *38*, 7536–7539.
(18) (a) Yamamoto, K.; Ito, E.; Fukaya, S.; Takagi, H. *Macromolecules* **2009**, *42*, 9561–9567. (b) Tobis, J.; Thomann, Y.; Tiller, J. C. *Polymer* **2010**, *51*, 35–45. (c) Subramanyam, U.; Kennedy, J. P. *J. Polym. Sci., Part A: Polym. Chem.* **2009**, *47*, 5272–5277.
(19) (a) Lin, C.; Gitsov, I. *Macromolecules* **2010**, 43, 3256−3267. (b) Bartels, J. W.; Billings, P. L.; Ghosh, B.; Urban, M. W.; Greenlief, C. M.; Wooley, K. L. *Langmuir* **2009**, *25*, 9535–9544.
(20) Triftaridou, A. I.; Kafouris, D.; Vamvakaki, M.; Georgiou, T. K.; Krasia, T. C.; Themistou, E.; Hadjiantoniou, N.; Patrickios, C. S. *Polym. Bull.* **2007**, *58*, 185–190.
(21) Webster, O. W.; Hertler, W. R.; Sogah, D. Y.; Farnham, W. B.; RajanBabu, T. V. *J. Am. Chem. Soc.* **1983**, *105*, 5706–5708.
(22) Chiefari, J.; Chong, Y. K.; Ercole, F.; Krstina, J.; Jeffery, J.; Le, T. P. T.; Mayadynne, R. T. A.; Meijs, G. F.; Moad, C. L.; Moad, G.; Rizzardo, E.; Thang, S. H. *Macromolecules* **1998**, *31*, 5559–5562.
(23) (a) Wang, J. S.; Matyjaszewski, K. *J. Am. Chem. Soc.* **1995**, *117*, 5614–5615. (b) Kato, M.; Kamigaito, M.; Sawamoto, M.; Higashimura, T. *Macromolecules* **1995**, *28*, 1721–1723.
(24) Achilleos, M.; Legge, T. M.; Perrier, S.; Patrickios, C. S. *J. Polym. Sci., Part A: Polym. Chem.* **2008**, *46*, 7556–7565.
(25) Triftaridou, A. I.; Vamvakaki, M.; Patrickios, C. S. *Biomacromolecules* **2007**, *8*, 1615–1623.
(26) Triftaridou, A. I.; Loizou, E.; Patrickios, C. S. *J. Polym. Sci., Part A: Polym. Chem.* **2008**, *46*, 4420–4432.
(27) Simmons, M. R.; Yamasaki, E. N.; Patrickios, C. S. *Macromolecules* **2000**, *33*, 3176–3179.
(28) Triftaridou, A. I.; Hadjiyannakou, S. C.; Vamvakaki, M.; Patrickios, C. S. *Macromolecules* **2002**, *35*, 2506–2513.
(29) Vamvakaki, M.; Patrickios, C. S. *Chem. Mater.* **2002**, *14*, 1630–1638.
(30) Achilleos, D. S.; Georgiou, T. K.; Patrickios, C. S. *Biomacromolecules* **2006**, *7*, 3396–3405.
(31) Achilleos, M.; Krasia-Christoforou, T.; Patrickios, C. S. *Macromolecules* **2007**, *40*, 5575–5581.
(32) Krasia, T. C.; Patrickios, C. S. *Macromolecules* **2006**, *39*, 2467–2473.
(33) Vamvakaki, M.; Patrickios, C. S.; Lindner, P.; Gradzielski, M. *Langmuir* **2007**, *23*, 10433–10437.
(34) Georgiou, T. K.; Patrickios, C. S.; Groh, P. W.; Iván, B. *Macromolecules* **2007**, *40*, 2335–2343.
(35) Hadjiantoniou, N. A.; Patrickios, C. S. *Polymer* **2007**, *48*, 7041–7048.
(36) Vamvakaki, M.; Patrickios, C. S. *Soft Matter* **2008**, *4*, 268–276.
(37) Kafouris, D.; Gradzielski, M.; Patrickios, C. S. *Macromolecules* **2009**, *42*, 2972–2980.
(38) Hadjiantoniou, N. A.; Patrickios, C. S.; Thomann, Y.; Tiller, J. C. *Macromol. Chem. Phys.* **2009**, *210*, 942–950.
(39) Rikkou, M. D.; Loizou, E.; Porcar, L.; Butler, P.; Patrickios, C. S. *Macromolecules* **2009**, *42*, 9412–9421.
(40) Rikkou, M. D.; Loizou, E.; Porcar, L.; Patrickios, C. S. *Eur. Polym. J.* **2010**, *46*, 441–449.
(41) Rikkou, M. D.; Kolokasi, M.; Matyjaszewski, K.; Patrickios, C. S. *J. Polym. Sci., Part A: Polym. Chem.* **2010**, *48*, 1878–1886.
(42) Kali, G.; Georgiou, T. K.; Iván, B.; Patrickios, C. S.; Loizou, E.; Thomann, Y.; Tiller, J. C. *Macromolecules* **2007**, *40*, 2192–2200.
(43) Kali, G.; Georgiou, T. K.; Iván, B.; Patrickios, C. S.; Loizou, E.; Thomann, Y.; Tiller, J. C. *Langmuir* **2007**, *23*, 10746–10755.
(44) Kali, G.; Georgiou, T. K.; Iván, B.; Patrickios, C. S. *J. Polym. Sci., Part A: Polym. Chem.* **2009**, *47*, 4289–4301.
(45) Bruns, N.; Tiller, J. C. *Macromolecules* **2006**, *39*, 4386–4394.
(46) Hu, Z.; Chen, L.; Betts, E. D.; Pandya, A.; Hillmyer, M. A.; DeSimone, J. M. *J. Am. Chem. Soc.* **2008**, *130*, 14244–14252.
(47) Powell, K. T.; Cheng, C.; Wooley, K. L.; Singh, A.; Urban, M. W. *J. Polym. Sci., Part A: Polym. Chem.* **2006**, *44*, 4782–4794.
(48) Krupers, M. J.; Möller, M. *J. Fluor. Chem.* **1997**, *82*, 119–124.
(49) Patton, D. L.; Mullings, M.; Fulghum, T.; Advincula, R. C. *Macromolecules* **2005**, *38*, 8597–8602.
(50) Jayalakshmi, R.; Ramadas, S. R.; Pillai, C. N. *Org. Prep. Proc. Int.* **1981**, *13*, 71–79.
(51) Inoue, Y.; Watanabe, J.; Takai, M.; Yusa, S.-I.; Ishihara, K. *J. Polym. Sci., Part A: Polym. Chem.* **2005**, *43*, 6073–6083.
(52) Patrickios, C. S.; Hertler, W. R.; Abbott, N. L.; Hatton, T. A. *Macromolecules* **1994**, *27*, 930–937.
(53) Lowe, A. B.; Billingham, N. C.; Armes, S. P. *Chem. Commun.* **1997**, 1035–1036.
(54) Philippova, O. E.; Hourdet, D.; Audebert, R.; Khokhlov, A. R. *Macromolecules* **1997**, *30*, 82–78−8285.
(55) Hadjiyannakou, S. C.; Yamasaki, E. N.; Patrickios, C. S. *Polymer* **2001**, *42*, 9205–9209.